Forest Ecology and Management 603 (2026) 123450

Contents lists available at ScienceDirect

Forest Ecology and Management

journal homepage: www.elsevier.com/locate/foreco

# Simulation of recurring defoliation by multiple insects shows lasting consequences for carbon storage in temperate oak forests

Jane R. Foster [a,1,*], Robert M. Scheller [a,2], Brian R. Sturtevant [b], Philip A. Townsend [a], Brian Miranda [c], David J. Mladenoff [a]

[a] Department of Forest and Wildlife Ecology University of Wisconsin-Madison, 1630 Linden Dr, Madison, WI 53706, USA
[b] USDA Forest Service Northern Research Station, Rhinelander, WI, USA
[c] USDA Forest Service Northern Research Station, La Crosse, WI, USA

ARTICLE INFO

*Keywords:*
Forest disturbance
Harvesting
Active management
Spongy moth
Forest tent caterpillar
LANDIS-II
*Lymantria dispar* L.
*Malacossoma disstria* Hbn

ABSTRACT

Insect defoliation outbreaks are dynamic forest disturbances that alter species composition and carbon balance. In the Central Appalachian Mountains, U.S.A., the invasive spongy moth (SM, *Lymantria dispar* L., formerly called gypsy moth) has been spreading and impacting oak forests for 45 years, yet much about how its outbreaks compound the effects of native defoliator inhabitants remains unknown. We developed a model to simulate insect defoliation and project long-term consequences on forest biomass and composition. The model incorporates outbreak spatial dynamics derived from Landsat data and implements species-specific tree-growth and mortality responses. We used this model with the LANDIS-II forest change model to simulate forest dynamics over 400 years in a managed forest in western Maryland, with and without SM defoliation, to quantify changes that follow invasion. Additional scenarios included a native defoliator, forest tent caterpillar (FTC, *Malacosoma disstria* Hbn.), to examine how multiple defoliators alter disturbance outcomes. Results showed that SM invasion changed forest species composition in unexpected ways. Shade tolerant species increased less after SM invaded, even though they were not preferred hosts, due to their proximity to neighboring host species. Forest carbon was temporarily reduced following individual outbreaks, and long-term aboveground C was lower (by 7.2 Mg C $ha^{-1}$ on average), with SM than without. Changes in forest aboveground C stocks were more pronounced when a native defoliator was included, particularly when outbreaks synchronized. Interacting insect disturbances have significant consequences for forest C storage and should be incorporated into our growing understanding of C dynamics at landscape scales.

## 1. Introduction

Temperate forests are subject to multiple disturbances that may interact with each other (Allen, 2007) and cause unexpected changes in forest structure (Peters et al., 2004, Lucash et al., 2018). Insect defoliation outbreaks play a significant role in disturbance regimes, with impacts that can be identified in tree-ring chronologies (Ryerson et al., 2003) and inferred from adaptations that allow tree species to coexist with native defoliators (Cooke and Lorenzetti, 2006, McCullough, 2000). Yet, non-native insects that can damage trees without natural defenses continue to be introduced to the U.S. (Niemelä and Mattson, 1996, Lovett et al., 2016, Liebhold et al., 2023) where they can alter disturbance dynamics. Changing environmental conditions may allow non-native populations to expand into new geographic areas (Volney and Fleming, 2000, Tobin et al., 2014), and some introduced defoliators spread steadily into favorable habitats (Sharov et al., 1999, Regniere et al., 2009) where their populations overlap with native defoliators. Compounded disturbances caused by the overlap of native and invasive defoliator populations have the potential to alter carbon (C) dynamics in oak forests, yet these effects are rarely quantified.

Many of the most damaging forest defoliators are moth species that emerge in the spring to feed when foliage is young, high in nutrients and low in defensive compounds (Herms and Mattson, 1992). Outbreaks of these spring defoliators have been shown to directly affect C uptake in

* Corresponding author.
*E-mail address:* Jane.Foster@usda.gov (J.R. Foster).
[1] (Present address) USDA Forest Service Southern Research Station, 2730 Cherokee Farm Way, Knoxville, TN 37920
[2] (Present address) Department of Forestry and Environmental Resources, North Carolina State University, Raleigh, NC, USA

https://doi.org/10.1016/j.foreco.2025.123450
Received 25 July 2025; Received in revised form 13 December 2025; Accepted 16 December 2025
Available online 23 December 2025
0378-1127/Published by Elsevier B.V.

forests by removing photosynthetic tissue in early summer, when canopy assimilation rates are highest, as demonstrated with $CO_2$ eddy covariance research in *Acer* and *Quercus-Pinus* dominated forests (Cook et al., 2008, Clark et al., 2010). Unlike discrete stand-replacing disturbances, defoliator outbreaks may extend over more than one growing season, causing persistent stress to trees (MacLean, 1980, Man and Rice, 2010). Defoliation that persists for multiple years reduces wood growth measured at tree and stand scales by 20–100 % (Foster, 2017) and increases mortality of preferred hosts (Fei et al., 2019), thus increasing respiration and reducing C accumulation and net ecosystem production (NEP) (Clark et al., 2010). Differential mortality may also change forest composition to favor non-host tree species (Davidson et al., 1999, Frey et al., 2023). Shifts in species composition could increase or decrease future C accumulation rates and C stocks, depending on the productivity and potential stature of favored tree species (Lichstein et al., 2009, Peltzer et al., 2010). Reduced host abundance may also dampen future defoliator outbreaks in ways that are only evident over long time-periods (McCullough, 2000, Cooke et al., 2024), allowing C stocks to recover.

Insect defoliation has been shown to shift forest ecosystems from net C sinks to C sources over individual outbreaks, as shown by Clark et al. (2010) who reported a 65 % reduction in NEP of *Quercus-Pinus* stands, yet defoliation effects on C sequestration remain poorly characterized over decades or centuries and at landscape scales (Cook et al., 2008, Quirion et al., 2021). Efforts have been made to quantify defoliation impacts on C dynamics over larger spatial domains using national forest inventory data. Fei et al. (2019) attempted to estimate an invasive defoliator's effects on county level C stocks by looking for variations in mortality, but they were unable to detect significant effects with inventory data alone. Rather, elevated mortality (of 2.4 % and >3.1 %) in that study could only be detected when independent data on persistent defoliation (of two or more years) were also available. Due to the ongoing need for defoliation data that could be linked to changes in forest carbon (Whitehead 2011), insect disturbances are generally absent from or inadequately represented in global vegetation models (Schimel, 2007, Pan et al., 2009, Pinkard et al., 2011, Fisher et al., 2015), even as the intensity and effects of these disturbances may be increasing (Peltzer et al., 2010).

Determining how novel disturbance regimes affect forest biomass, C storage, and species composition is a pressing research need that can be addressed with a simulation approach (Medvigy et al., 2012, Gustafson et al., 2018). Landscape models that bridge scales of observation provide an opportunity to quantify a range of possible C accumulation patterns that result from changing insect disturbances. We designed a defoliation model extension for the forest landscape model LANDIS-II (Scheller et al., 2007), to quantify the effects of periodic defoliation on forest biomass and species composition. Here, we demonstrate the model and its behavior to quantify how aboveground biomass in live and dead-wood changes when mixed oak forests experience periodic defoliation outbreaks in the Central Appalachians, U.S.A. We evaluated the hypothesis that defoliation caused by an introduced invasive defoliator, spongy moth (SM; formerly called gypsy moth) (*Lymantria dispar* L. 1758), would reduce aboveground forest C pools and accumulation rates in comparison to the alternative regime of forest harvest and a native defoliator, forest tent caterpillar (FTC) (*Malacosoma disstria* Hbn.1820). We examined changes in forest composition and asked whether spongy moth invasion reduced the dominance of its host tree species over time. Finally, we considered whether changes in C accumulation rates associated with insect disturbance represent trends capable of changing temperate forests from net carbon sinks to carbon sources (Houghton 2005, Pan et al., 2011).

## 2. Methods

### 2.1. Study area

SM invaded mixed oak forests in the Central Appalachian Mountains of eastern U.S.A in the early 1980s (Reardon et al., 1993). Green Ridge State Forest (GRSF) lies within this invasion zone in the Ridge and Valley physiographic region in western Maryland (MD). It is characterized by steep ridges that trend from Northeast to the Southwest (Fig. 1). Annual precipitation averages 1000 mm and is distributed evenly throughout the year. The mean annual temperature is 10.6° C, with average winter lows of −5.0° C and summer highs of 28° C. Soils at GRSF are mainly derived from shale or sandstone and are shallow to bedrock and well-drained (Mash, 1996). Elevation ranges from approximately 200–600 m a.s.l. The forests of GRSF were heavily cut over between 1880 and 1910 (Mash, 1996), producing a forest with a mean stand age of 75 years, and a maximum age over 150 years, in the year 2000 (Fig. C1). Forest composition at GRSF is dominated by oak mixtures that are representative of the central hardwoods region (Fig. 2). White oak (*Quercus alba* L. 1753) and scarlet oak (*Q. coccinea* Munchh.) are both prominent on lower slopes and elevations. Red oak (*Q. rubra* L. 1753) and chestnut oak (*Q. montana* Willd. 1805) are abundant on ridges and rocky slopes, and black oak (*Q. velutina* L. 1785) is prevalent at mid slopes. A mix of pines, including Virginia pine (*Pinus virginiana* Mill. 1768) occur with white pine (*P. strobus* L. 1753) in deciduous mixes or pure stands and hemlock (*Tsuga canadensis* Carriere 1855) grows in drainages and on protected north-facing slopes.

We assumed that future disturbance regimes would include components of historic disturbances including wind and harvest. Typical wind damage events for the study area range in severity and size but are mostly constrained to smaller patch-sizes by the rugged, steep topography. Over half of GRSF has been designated for active forest management. Forest harvest plans circa 2000 aimed to sustain natural and recreational resources, but did not explicitly account for periodic SM outbreaks that followed invasion. FTC outbreaks were reported in nearby forests as recently 2007, a year when SM populations were also increasing in GRSF (J. Foster, personal observation). Other defoliators such as the looper complex (*Phigalia titea* Cramer 1782 and *Erannis tiliaria* Harris 1841) have also had outbreaks at GRSF, as reported for 1981 (Crow and Hicks, 1990). Increasing defoliation outbreaks could interact with harvest regimes to change forest composition from the desired *Quercus-Pinus* mixes to some other endpoint, with unknown consequences for future harvest and conservation goals (James et al., 2007). Historical fire statistics for Allegany County suggest that fire occurrence was higher when human exploitation of the forest was most intense in the early 1900s (Mash, 1996), but fires have become increasingly rare and are generally suppressed (MTBS data, Picotte et al., 2020). In contrast to previous applications of this model in the same region (Gustafson et al., 2017, 2018), this study isolates the long-term consequences of defoliator disturbances and their interactions on live and dead-wood carbon and biomass dynamics.

### 2.2. Model Description

LANDIS-II is a spatially interactive forest succession and disturbance model frequently used to understand the effects of disturbances on forest landscapes (Scheller et al., 2007), that has evolved from the original LANDIS model (Mladenoff, 2004). It operates on a raster grid, with tree-species cohort-level growth, mortality, competition, and establishment occurring within grid cells, and spatial processes such as dispersal and disturbance spreading among grid cells. Each grid cell can be populated by cohorts of multiple species that respond to local conditions, competition and disturbance based on life history traits (Appendix B, Table B1). Species may be represented by many age-cohorts in a grid cell, which allows diverse stand dynamics. Modular model extensions to simulate succession or forest disturbances and can be used individually

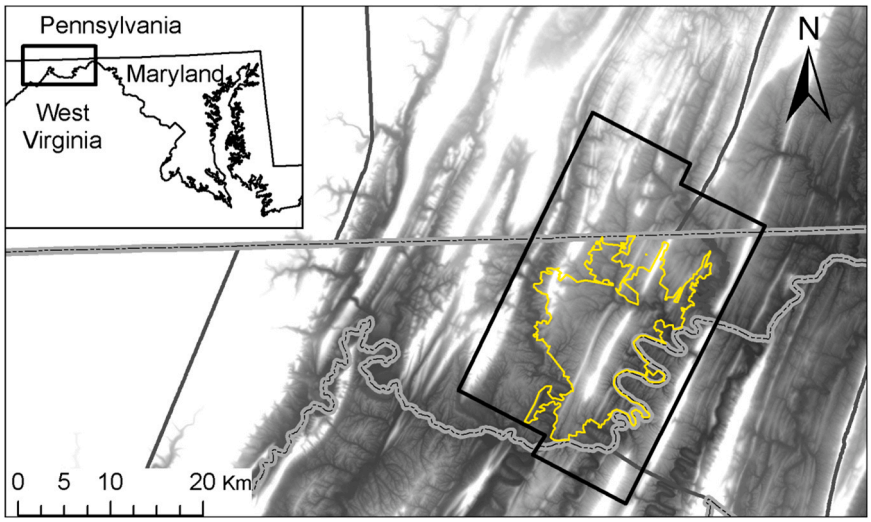


**Fig. 1.** Green Ridge State Forest in Allegany County, Maryland, USA (forest boundaries in yellow) (78.473 W, 39.623 N). Black box delimits simulation extent (~22 km by 33 km). Elevation ranges from approximately 200 m A.S.L (dark grey) to 600 m A.S.L. (white). Map lines delineate study areas and do not necessarily depict accepted national boundaries.

or in combination to approximate historic or novel disturbance regimes. The Biomass Succession model extension simulates processes of forest succession including spatially dynamic seed dispersal, and aspatial growth and mortality. The model tracks accumulation and changes in aboveground live and dead woody-biomass pools at each grid cell and for each species cohort (Scheller and Mladenoff, 2004). It is derived from the original LANDIS model that was based on age cohorts alone (now deprecated) and is one of many successional models that each represent forest stocking or biomass and carbon pools in different ways (Mladenoff et al., 1996; Mladenoff and He, 1999, Mladenoff, 2004, Wang et al., 2015, Gustafson et al., 2017). Briefly, with the Biomass Succession model, a cohort growing without competition can increase in biomass each year up to a species-specific maximum aboveground net primary productivity (ANPPmax) parameter value and the algorithms described by Scheller and Mladenoff (2004). Cohort biomass growth is further modified by the presence of competing cohorts in the same grid-cell (competition), and by stochastic disturbances that may directly or indirectly cause growth to change or mortality to occur for one or many cohorts (Scheller and Mladenoff, 2004). ANPPmax parameters are modeled separately and when carefully parameterized the Biomass Succession model can reproduce aboveground biomass dynamics within 1 % of empirical observations (Reese et al., 2024, Simons-Legaard et al., 2025).

To model changes in aboveground biomass related to defoliation, we developed an insect disturbance model extension and tested its behavior with LANDIS-II Biomass Succession extension v2. The purpose of this model extension, named 'Biomass Insects', is to simulate landscape-level defoliation events and their effects on forest cohort growth and mortality. While versions of this extension have been applied to test applied research questions and different implementations with LANDIS-II (Kretchun et al., 2014, Gustafson et al., 2017, 2018, Lucash et al., 2018), this is the first study to fully describe the model's behavior as originally designed by Foster (2011) and to demonstrate the specific effects of defoliation outbreaks on both live and dead-wood carbon dynamics. 'Biomass Insects' simulates defoliator outbreaks with spatial and temporal patterns of defoliation intensity that are derived empirically from Landsat defoliation maps (Foster et al., 2013). The extension simulates the initiation of an outbreak by growing defoliated patches in susceptible forest areas until two metrics approximate observed outbreak patterns. These metrics are: 1) the distribution of disturbed patch-sizes and 2) the mean landscape defoliation, (Foster et al., 2013, Appendix A). Modeled defoliation intensity varies within patches and can spread among patches over the duration of an outbreak. The model stochastically triggers periodic outbreaks with a frequency and duration that can be tuned to each defoliator species' observed temporal patterns. When outbreaks are triggered, the model distributes defoliation within a grid-cell based on the insects' host-preferences and modifies cohort growth and mortality based on tree species-specific relationships from the defoliation impact literature (Foster, 2017, Appendix A). 'Biomass Insects' can simulate multiple defoliators on an annual basis and is compatible with different LANDIS-II succession and disturbance extensions, including more general biological disturbance extensions (-e.g., Sturtevant et al., 2004).

Defoliator outbreaks are cyclic-eruptive; characterized by periodic fluctuations of insect populations that occasionally lead to extensive damage (Cooke et al., 2007, Cooke et al., 2024). 'Biomass Insects' approximates temporal patterns characteristic of population fluctuations by drawing from two empirical distributions that are specific to each defoliator: 1) a distribution of the typical number of years that pass between outbreaks (inter-outbreak interval) and 2) a distribution of outbreak length or duration in years (Fig. 3) (Cooke and Lorenzetti, 2006, Johnson et al., 2005, Johnson et al., 2006). Inter-outbreak interval is assumed to be normally distributed, while outbreak duration is defined by a modified negative exponential distribution, such that shorter outbreaks are more common than long ones (Wood, 2008, Cooke et al., 2009).

When an outbreak occurs, insect defoliation removes a fraction of leaf biomass from the forest canopy and transfers remnants of it to the forest floor. We defined defoliation intensity as the fraction of leaf biomass that is removed by defoliator populations during a single growing season. The model tracks defoliation at the cohort and grid-cell scale and reduces annual growth of each species-cohort by the proportion of modeled defoliation intensity that it experiences (See Appendix A: Defoliation Impacts: Growth and Mortality Responses for more details). We defined defoliation severity to be the amount of wood (in biomass) transferred from the live to dead wood pools due to mortality caused by defoliation and the model tracks the biomass of partial mortality attributable to each defoliator species in units of mass. Tree species differ in their susceptibility to defoliation, which is represented in the model by up to three categorical susceptibility classes (with 1 being most susceptible) that vary by insect species. The defoliation intensity experienced by a cohort in an outbreak year therefore depends on the cohort's susceptibility class, the mean susceptibility of all the species-cohorts in the same grid cell, and the defoliation experienced in the

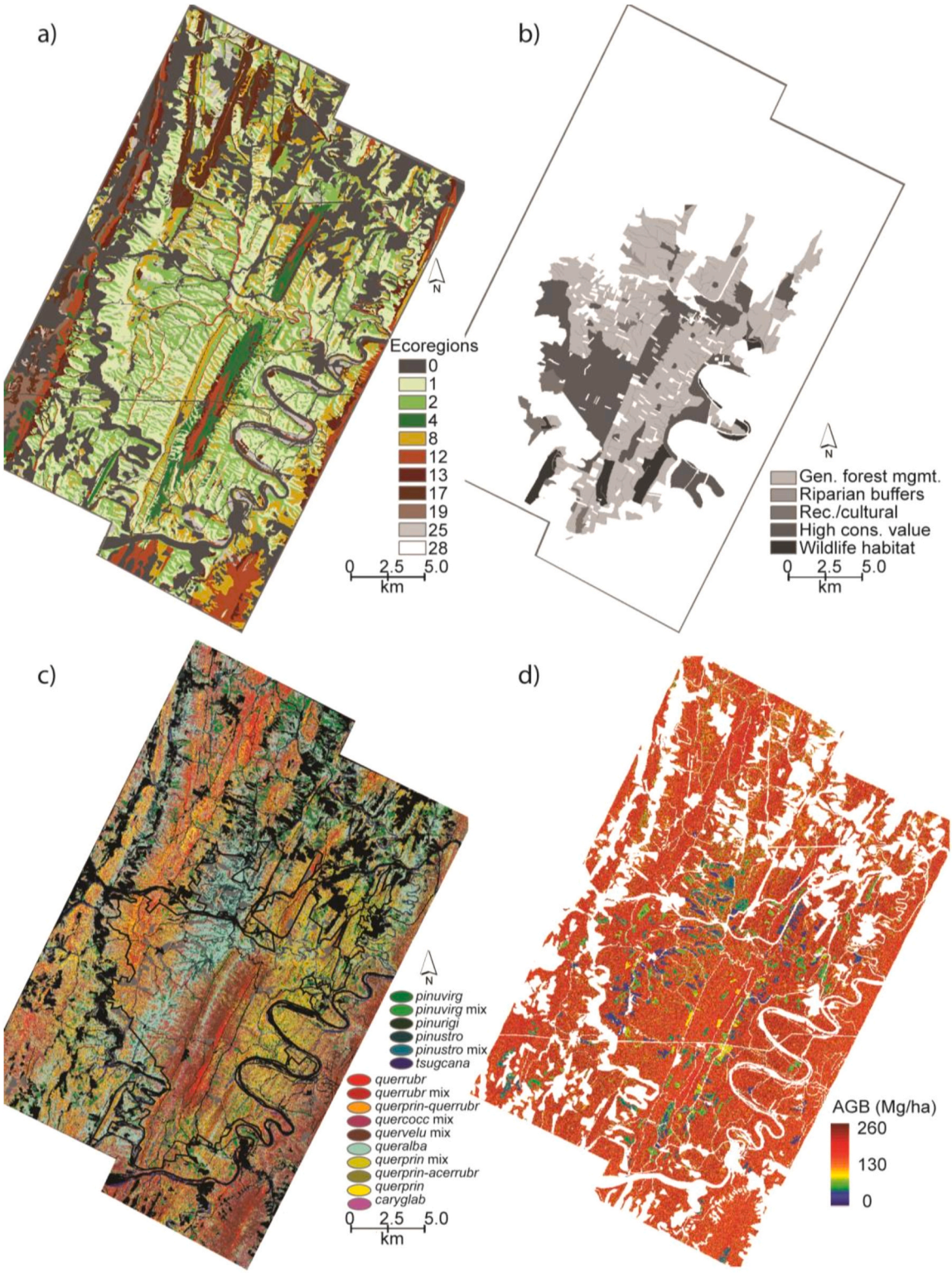


**Fig. 2.** Landis-II input maps of soil and climate ecoregions (a), GRSF management zones (b) forest cover type (c), and initial live aboveground biomass (AGB) in year 0 (2000).

previous year by nearby forested grid cells, calculated as a mean over a specified neighborhood area. Outbreak initiation and spread mimics the spatial patterns observed from satellite image disturbance maps (Foster et al., 2013, Appendix A). Additional model details are available in Appendix A.

### 2.3. Simulation experimental design

We implemented 'Biomass Insects' for the GRSF landscape to test how recurring defoliator outbreaks affect forest composition and aboveground C storage. We included wind, forest harvesting, and insect defoliation in our simulation experiment. We excluded fire because the future fire regime is uncertain and subject to ongoing suppression from

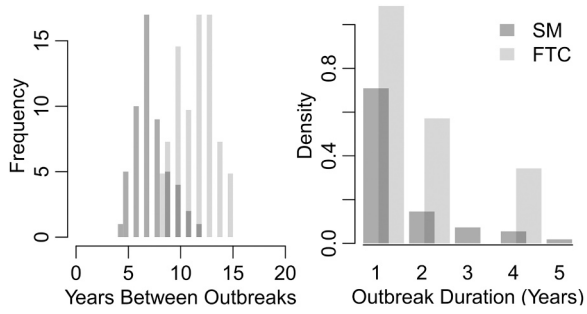


**Fig. 3.** Temporal characteristics of spongy moth (SM) and forest tent caterpillar (FTC) outbreaks that result from the parameters and the 'Biomass Insects' model for one replicate simulation run over 400 years. SM outbreaks were modeled to be more frequent, with longer duration on average than FTC, based on the literature as described in the Methods section.

forest management agencies. Wind events were parameterized to reach a typical maximum size of 100 ha with a moderately frequent return period of 500–700 years for all wind events of any severity (Xu et al., 2012, Appendix B, Table B2). These return intervals mean that over 500 years wind events of some severity would occur over an area equivalent to the study area, and the most severe wind events would recur every 13,000 years. We simulated harvest disturbance with the Base Harvest (v1.3) model extension and incorporated management prescriptions designed to mimic the management plan from 2011 and associated map data for GRSF (M. Beals, Forest Manager GRSF, personal communication). We treated harvest and wind as background disturbances and therefore included both in all scenarios (Table 1). Three defoliation scenarios reflected potential disturbance regimes that incorporate introduced SM outbreaks, native FTC outbreaks, or a combination of both SM and FTC together. Five replicate simulations were run for 400 years with annual time-steps starting in the year 2000 for each of four scenarios (Table 1): 1) control = wind + harvest, 2) control + FTC, 3) control + SM, 4) control + FTC + SM. We ran individual simulations with no disturbance and only wind disturbance to evaluate baseline model performance. The number of forest cells (>500,000), resolution (30 m x 30 m), and duration (400 years) dictated the number of replicates.

### 2.4. Model input data and parameterization

#### 2.4.1. Disturbance regimes

We patterned defoliator outbreaks after spatial and temporal characteristics of SM and FTC disturbances (Table 2). We set the mean inter-outbreak period to 7 years (standard deviation (SD)= 1) for SM (averaging periodicity reported in Allstadt et al., 2015) and 11 years (SD=2) for FTC (Johnson et al., 2006, Cooke et al., 2009). Outbreaks were limited to a maximum duration of five years for both defoliators, and FTC outbreaks tended to range from 1 to 3 years while SM outbreaks were occasionally longer (Fig. 3). Because FTC larvae emerge and begin feeding earlier in the spring than SM larvae, FTC defoliation always occurred before SM defoliation in a given year, such that if outbreaks overlapped, SM could only defoliate the amount of foliar biomass remaining after FTC activity.

We derived spatial input-parameters for SM outbreaks from analysis of the SM defoliation observed at GRSF in 2000–2001 (Foster et al., 2013). We calibrated model parameters to constrain SM outbreaks to the range of mean defoliation (~11–25 %) (Table 2). For FTC outbreaks, we modified SM spatial parameters to reflect the assumption that FTC would have smaller mean patch sizes as outbreak reports have been infrequent in the past decades (e.g. regional outbreaks have only been reported in 1969–72 and 1993–94). We also assumed that FTC would have a larger neighborhood size as FTC adults are better dispersers than SM (Mason and McManus, 1981, Peltonen et al., 2002) (Table 2). We varied tree species defoliation response parameters by tree functional groups that differ in xylem anatomy and leaf longevity including deciduous ring-porous and diffuse-porous species, and evergreen coniferous species based on Foster (2017). Host preference classes for SM followed Liebhold et al. (1995) while FTC preferences come from other sources (Parry and Goyer, 2004, Schowalter, 2017) and local state extension (Pennsylvania Department of Conservation and Natural Resources n.d.e). SM is a generalist with a broad diet and a strong preference for oaks, while FTC is restricted exclusively to broadleaf genera, with strong regional variation in host preference. Thus simulated SM and FTC defoliator outbreaks differed in temporal and spatial dynamics, and in host preference (Table 2, Appendix A).

We included planned harvesting regimes as baseline disturbances in all scenarios (M. Beals, personal communication). Management units were based on the management map for GRSF (MD DNR January 2011, Fig. 2b). Harvest prescriptions were limited to areas designated for active timber management, comprising 57 % of approximately 19,100 ha (Fig. 2b). Prescriptions ranged from salvage cuts of senescing pine and black locust to white pine release and pre-commercial thinning of mixed oaks (Appendix B, Table B3). The model targeted 1 % of the

**Table 1**
Simulation experiment scenarios. Wind and harvesting were considered background disturbance regime. Scenarios with no disturbance or only wind disturbance showed little variation among replicates and were run primarily to check model behavior.

| Scenario | Replicates | Disturbances | | | |
|---|---|---|---|---|---|
| | | Wind | Harvest | FTC | SM |
| No Disturbance | 1 | - | - | - | - |
| Wind | 1 | X | - | - | - |
| Control | 5 | X | X | - | - |
| Control + FTC | 5 | X | X | X | - |
| Control + SM | 5 | X | X | - | X |
| Control + FTC + SM | 5 | X | X | X | X |

**Table 2**
LANDIS-II biomass defoliation extension input parameters. See Appendix B for more details on specific parameters.

| | Defoliator | | |
|---|---|---|---|
| Input parameters | Spongy moth | Forest tent caterpillar | |
| Mean duration rate | 0.8 | 1.8 | |
| Time between outbreaks (years) | 7 (1) | 11 (2) | |
| Mean (sd) | | | |
| Neighborhood size (m) | 100 | 150 | |
| Initial area calibration | $8 \times 10^{-5}$ | $6 \times 10^{-5}$ | |
| Initial patch distribution | Weibull | Weibull | |
| Initial patch value 1 | 1.1 | 1.1 | |
| Initial patch value 2 | 350 | 250 | |
| Growth reduction parameters (slope, intercept) | | | |
| Diffuse porous species | -0.80, 1 | -0.80, 1 | |
| Ring porous species | -0.16, 1 | -0.16, 1 | |
| Coniferous species | -1.00, 1 | -1.00, 1 | |
| Mortality parameters (m, b) | | | |
| Diffuse porous species | 0.009, 7 | 0.009, 7 | |
| Ring porous species | 0.006, 5.5 | 0.006, 5.5 | |
| Coniferous species | 0.016, 4 | 0.016, 4 | |
| Host type$^{\varphi}$ | Neighborhood defoliation | | |
| | Beta parameters (1, 2) | | |
| | 0–20 % | 20–40 % | 40–100 % |
| Preferred (1) | (0.29, 4.12) | (1.17, 2.64) | (1.06, 0.81) |
| Resistant (2) | (0.26, 4.92) | (0.76, 2.13) | (0.73, 0.75) |
| Immune (3) | (0.25, 6.09) | (0.65, 1.66) | (0.51, 1.01) |

$\varphi$ Neighborhood defoliation is calculated each outbreak year for each grid-cell and used to look-up Beta distribution parameters for random draws of the defoliation intensity experienced by grid-cell cohorts of each host type. These parameters were the same for SM and FTC. The mean annual defoliation realized on each grid-cell is calculated as the biomass weighted mean of defoliation across all cohorts and thus depends on local host abundance that is dynamic through time.

managed area for harvest per year on average to produce the planned 100-year rotation. Individual harvest events were constrained by stand boundaries and followed a patch size distribution corresponding to a Weibull distribution (shape ~ 1.18, scale ~ 6.5) with a median harvest area of 5 ha.

#### 2.4.2. Initial forest composition and age map

The LANDIS-II model requires an input raster map of initial forest composition that specifies the species and cohort ages that occupy each grid cell in the landscape. We derived the initial forest conditions from analysis of airborne hyperspectral imagery from AVIRIS (updated from community analysis methods in Foster and Townsend 2004), maps of harvest polygons dating from 1969 to 2000 (Maryland Department of Natural Resources (MD DNR)), and continuous forest inventory (CFI) data from a systematic network of 436 plots sampled by the MD DNR in 1999 and 2000. The resulting forest community type map represented 18 forest classes made up of 24 species (Appendix B, Table B1). CFI plots and associated species data were randomly assigned to each raster grid cell in the map according to forest community type membership. This approach resulted in assignment of 522 unique initial forest communities. Non-forest land uses, including roads, agricultural fields, and water bodies were masked and inactive during simulations, leaving 52,881 ha active in the model.

#### 2.4.3. Soil ecoregions and species establishment

Species growth and establishment varied across the landscape in relation to ecoregions that were derived to represent homogenous soil and climate conditions. We derived a soil ecoregions raster from the Soil Survey Geographic Database (SSURGO) (Soil Survey Staff, 2009). Classes were differentiated based on seven soil variables: field capacity (water, 1/3 bar), wilting point (water, 15 bar), available water capacity, silt, sand, and clay content (%), and soil pH. Each soil property was averaged up to a soil depth of 40 cm (mean soil depth 36.7 cm) (Appendix B, Table B2). We used mean monthly maximum and minimum temperatures, precipitation, field capacity, wilting point, and base soil nitrogen of a given ecoregion to estimate the probability that a species cohort will establish on a grid-cell over a given time-period using the same combination of factors that drive establishment in the Linkages ecosystem model (Gustafson et al., 2010, Scheller and Mladenoff, 2005, Pastor and Post, 1985).

Succession in the Biomass Succession model results from competition among species that is driven by differences in life-history traits, existing cohort ages and aboveground biomass (AGB), and annual growth rates (calculated as a function of ANPPmax). We estimated ANPPmax for each species and ecoregion combination using a version of the PnET-II ecosystem process model that has been modified to be more responsive to differences in leaf mass area (Aber and Federer, 1992, Scheller and Mladenoff, 2004). ANPPmax derived from PnET-II averaged 789 g $m^{-2}$ $yr^{-1}$ (7.9 Mg $ha^{-1}$ $yr^{-1}$) across all species and ecoregions at GRSF, and ranged from a minimum of less than 400 g $m^{-2}$ $yr^{-1}$ for *P. virginiana* to over 1050 g $m^{-2}$ $yr^{-1}$ for *Liriodendron tulipifera* L. 1753. These values agreed well with the range of ANPP values (~500–1000 g $m^{-2}$ $yr^{-1}$) measured empirically from tree rings and modeled by the ecosystem model PnET-CN for nearby forests (Davis et al., 2009, Dye et al., 2016). During initialization, the Biomass Succession extension grows the forest, starting with the oldest cohorts, until it reaches the initial age for each cohort based on the species, ages, and ANPPmax as specified for the initial communities. We evaluated our input maps and growth parameters by comparing the distribution of biomass values produced by this initial forest growth process with empirical biomass observed from the CFI plot dataset (Appendix C, Fig. C1). Following model initialization, the simulated mean AGB (145.2 Mg ha-$^{1}$) did not differ significantly from the inventory mean in 2000 (142.9 Mg ha-1, P = 0.56) (Fig. C1 a & b). We evaluated modeled live biomass growth rates from the control scenario by comparing them to live biomass increments from US Forest Inventory and Analysis (FIA) data for Allegany County, MD, and found that mean modeled growth (1.31 Mg $ha^{-1}yr^{-1}$, 95 % CI [1.27,1.35]) did not differ significantly from observed growth (mean 1.39 Mg $ha^{-1}yr^{-1}$, 95 % CI of [0.98, 1.80]) between 2010 and 2024 (Appendix C, Fig. C4).

### 2.5. Model output data analysis

We compared disturbance scenario means for the whole landscape for multiple output variables using ANOVAs and Tukey's Honestly Significant Difference (HSD) when F-tests proved significant. The variables tested included: total aboveground biomass (AGB) (live + dead woody pools), live AGB only, median cohort age, live relative biomass of the most abundant tree species, and the live relative biomass of the host tree species preferred by spongy moth. We also calculated aboveground biomass increment (AGBi), i.e. the rate of woody biomass accumulation in the landscape, as the instantaneous slope of the total AGB time series (e.g. total AGB = live + dead AGB) and compared rates of change among disturbance scenarios. AGBi can parallel temporal patterns in net primary productivity (NPP) and NEP in temperate forests (Luyssaert et al., 2007), though it is not equivalent. We examined results in terms of dry biomass (AGB) and aboveground C pools (Mg C $ha^{-1}$) (Thomas and Malczewski, 2007). Spongy moth host-dominance was measured at year 0, 50, 200, and 400 by summing maps of species biomass based on SM host-preference class and calculating the area of forest dominated by each class. We compared the area dominated by species preferred by SM over time and among scenarios. To evaluate the effect of harvests on forest biomass and composition, we compared scenario means between forests within and outside of GRSF boundaries (Fig. 2).

We evaluated the sensitivity of our simulation results to model parameters using a representative subset of the study landscape and the SM scenario (Appendix C, Table C4). We perturbed input parameters by + /- 10 %, except in cases where larger perturbations were necessary to produce meaningful changes in model behavior (e.g. neighborhood size was perturbed by length increments > the diagonal of a grid cell, while time-between-outbreaks was perturbed by whole year integers). We tested the sensitivity of our results to the landscape configuration of hosts by perturbing the host susceptibility classes of simulated tree species. We compared mean live and total AGB, dead wood pools, mean age and defoliation from each perturbed replicate with the base SM simulation results.

## 3. Results

### 3.1. Model behavior – 'Biomass Insects' defoliation model

The 'Biomass Insects' model created defoliator outbreaks for SM and FTC according to the temporal and spatial input parameters. Defoliation patches varied in size and shape (Fig. 4) and produced heterogeneous defoliation intensity. Outbreaks of FTC and SM occasionally overlapped in space and time (Fig. 4e). Overlap of outbreaks had the effect of increasing local intensity and severity, particularly if an earlier outbreak had already caused enough stress to induce significant mortality (Fig. 5).

Patchy defoliation produced mean landscape defoliation-intensity that ranged from 8 % to 22 % for SM outbreaks that varied in duration (Fig. 5). During the first 180 years, SM defoliation tended to increase in intensity over the course of an outbreak, as driven by the high initial host abundance in the landscape (Fig. 5a). Later, SM intensity was significantly lower after forest composition had changed enough to diminish the dominance of SM host species. As host abundance decreased over time, the model shifted its random draws of defoliation intensity from the highest intensity distributions to lower intensity distributions (Appendix A, Fig. A1). FTC outbreaks declined in intensity over the years of an outbreak throughout the course of the simulation, most likely because FTC hosts started out less abundant in the GRSF landscape (<33 % at year zero). FTC outbreaks were also less connected, which dampened the potential for neighborhood effects to spread

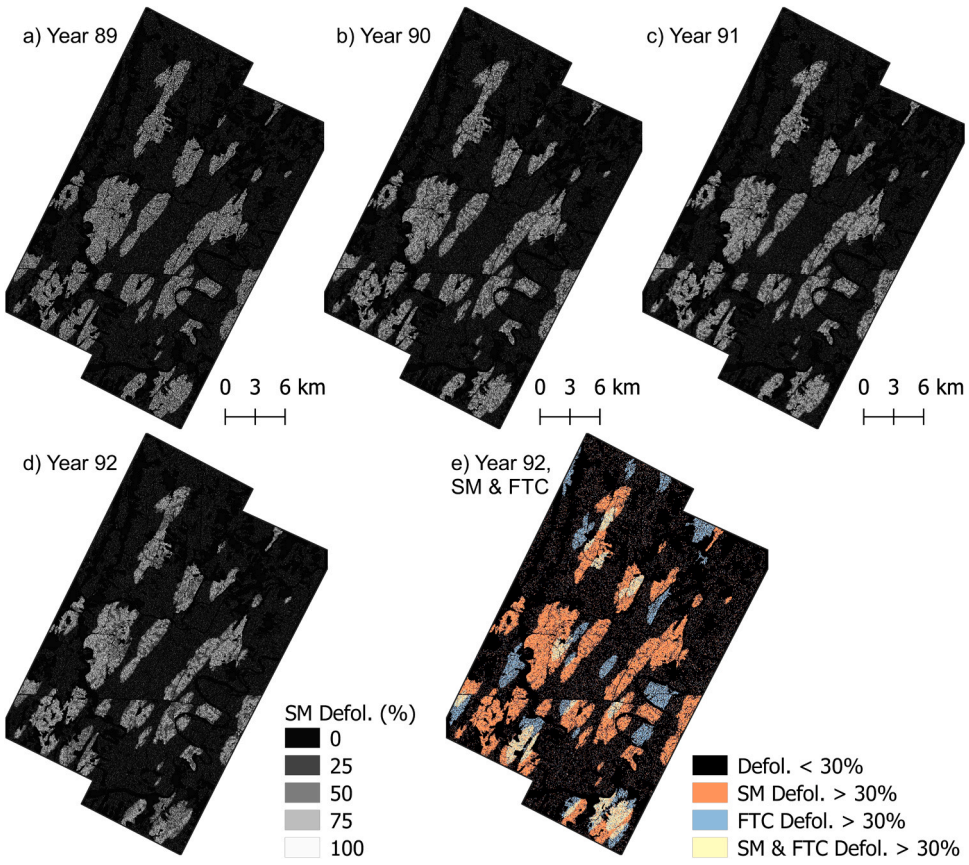


**Fig. 4.** Defoliation intensity maps for a simulated SM outbreak for years 89–92 (a-d) from a single replicate simulation, and showing overlap with a FTC outbreak in the final year (92) (e). Panels a through d show SM defoliation from 0 % to 100 % of canopy foliage in each grid cell. In the final panel (e), SM defoliation is displayed in orange, FTC defoliation displayed blue, and spatial overlap appears yellow.

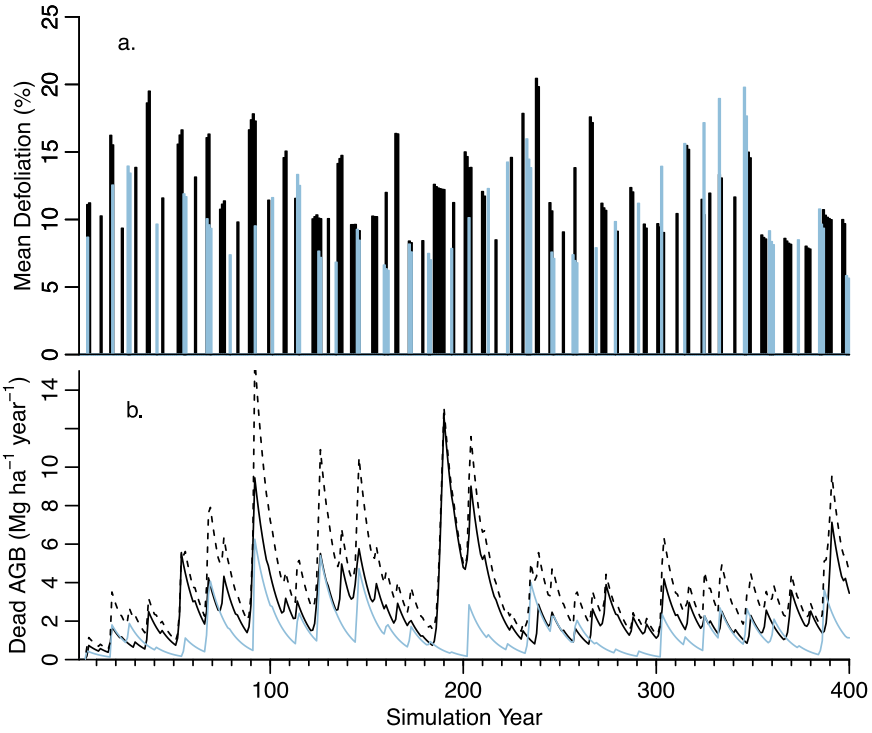


**Fig. 5.** Landscape mean defoliation (a) for outbreaks caused by FTC (light blue bars and lines) and introduced SM (black bars and lines) from one replicate simulation (the same used for Fig. 4) and (b) the dead aboveground biomass produced by each defoliator individually and combined (total insect related mortality shown with dashed line).

defoliation contagiously, despite the superior dispersal abilities of FTC.

Aboveground biomass responded to defoliator outbreaks with pulses of mortality that transferred woody biomass from the living to the dead wood pools (Fig. 5b). Landscape average mortality from defoliation was as high as 15 Mg ha$^{-1}$, but typically averaged less than 5–10 Mg ha$^{-1}$. Longer SM outbreaks resulted in the largest pulses in mortality, in agreement with mortality relationships that increase exponentially with accumulated defoliation (Foster, 2017, Appendix A). Occasionally, single year FTC outbreaks overlapped with the end of longer SM outbreaks and resulted in high mortality pulses. An example of this can be seen in the pulse of mortality at year 93 in Fig. 5b. Though the FTC outbreak only lasted one year (year 92, Fig. 5a), because it overlapped with the final year of a four-year SM outbreak (year 89–92, Fig. 4 & Fig. 5) it led to significant cohort mortality. In comparison, an isolated single-year FTC outbreak in year 41 (Fig. 5a) resulted in negligible mortality (Fig. 5b).

### 3.2. Trends in biomass and species composition

Live aboveground biomass (AGB) followed patterns over time that relate to successional dynamics. We illustrate this with examples showing how live and dead biomass changes both within individual grid cells (Fig. 6) and when averaged across the landscape (Fig. 7). In the absence of disturbance (Fig. 6a), AGB increased as the initial stand matured (from mean age ~ 70 in 2000) and increased in biomass. Dead AGB increased in proportion with live biomass. After the first century, mortality increased as cohorts approached their species' maximum age. This gradual senescent mortality caused AGB to steadily decrease to a simulation minimum around year 200 (Fig. 6 & Fig. 7). Mortality also released growing space for the establishment of new cohorts or the release of suppressed cohorts. Ingrowing cohorts were often more shade tolerant and therefore able to assume dominance of the released growing space. Harvests interrupted this pattern by periodically removing significant live AGB and leaving small amounts of dead woody biomass behind (Fig. 6c&d), while defoliation resulted in less mortality but left a larger proportion of dead biomass on the grid cell to accumulate and decay (Fig. 6b & 6d). The dead woody biomass pool declined over time due to diminished inputs until the surviving and newly established cohorts matured to large enough stature to replenish it again. In the harvested example site, AGB returned to a similar level following repeated harvests (Fig. 6c).

Grid cell scale dynamics followed a different trajectory when subjected to a combination of forest harvests and insect outbreaks of both SM and FTC (Fig. 6d). When defoliator outbreaks were long and intense,

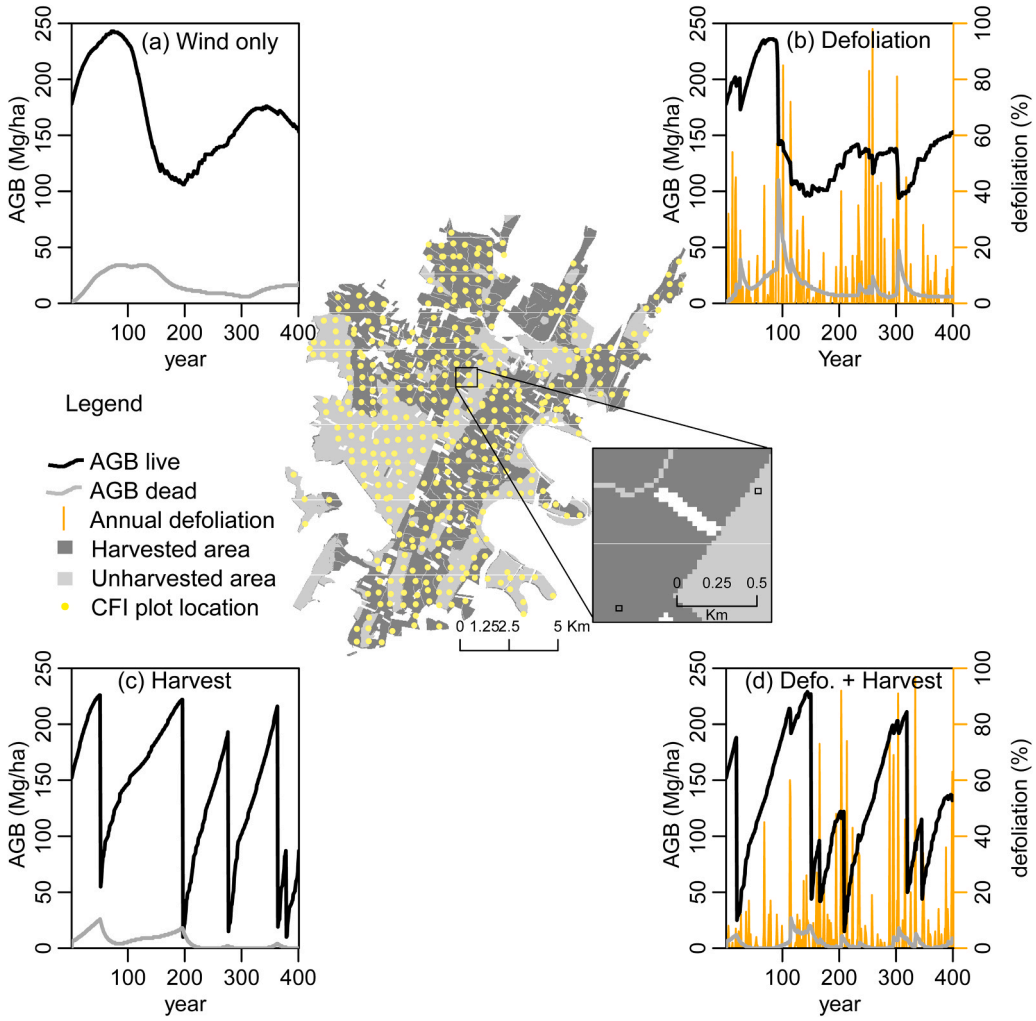


**Fig. 6.** Development of live and dead AGB at two individual grid-cells in managed and un-managed areas under different disturbance scenarios. AGB trends in the unmanaged forest area (light grey) includes only wind disturbances (a, wind occurs in all scenarios), yet when periodic defoliation outbreaks occur, live AGB becomes more variable, decreasing sharply during outbreaks of the longest duration and more slowly with less severe outbreaks (b). Dead AGB spikes following outbreaks then declines as wood decays (b). In managed areas where forest harvests occur, live AGB is periodically reduced when mature trees are harvested and dead AGB increases only a small amount as most harvested wood leaves the forest (c). When the same grid-cell experiences defoliation outbreaks and harvests (d), it is harvested fewer times, presumably because it takes longer to reach merchantable conditions due to defoliation effects.

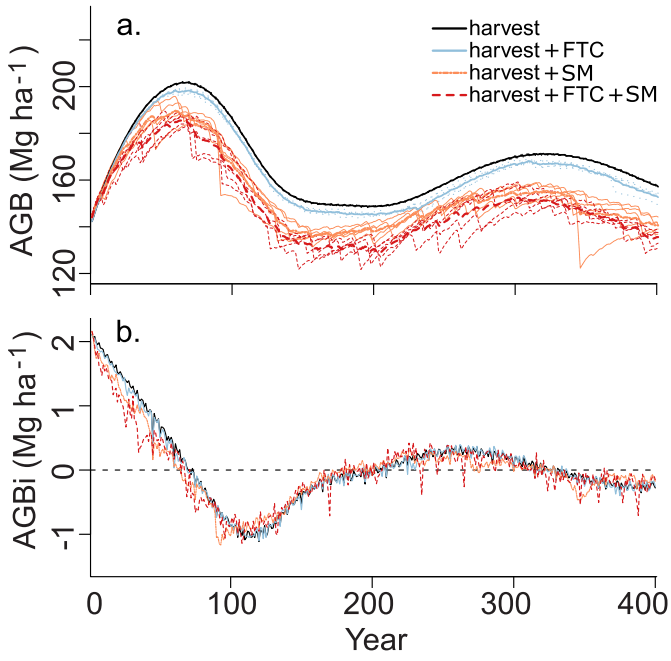


**Fig. 7.** Landscape means of live aboveground biomass (AGB) (a) for simulation replicates (thin lines) and scenario means (thick lines). Replicate simulations for the harvest control scenario are plotted, but vary too little to be visible around the mean. Scenario means of total aboveground biomass increment (AGBi) for the landscape (b) show the rate of biomass accumulation for the sum total of live and dead wood pools over time.

live-AGB dropped precipitously with a concurrent increase in dead biomass. While less severe outbreaks appeared to increase variability in live-AGB without a significant decrease in maximum live-AGB, defoliator outbreaks decreased the number of times that the site could be harvested, from four to three times, over 400 years (Fig. 6d).

When a site outside of the management zone (Fig. 6a) was subjected to FTC and SM defoliator outbreaks (Fig. 6b), live AGB declined by approximately 5–40 % due to defoliation mortality. Nonetheless, AGB appeared to approach the same level in the final 100 years as when no disturbances affected the site. The full landscape simulation contains wide variations on these dynamics occurring at each grid cell that may not be evident in landscape-means (Fig. 7a).

Carbon stored in landscape-mean aboveground biomass followed a similar pattern over time for all disturbance scenarios, for both C stored in live-AGB (Fig. 7) and in total biomass, or total-AGB C ((live + dead, not shown). Mean total-AGB C increased steadily over the first 65–70 years of the simulation, to maxima that ranged from 103 to 113 Mg C $ha^{-1}$ among scenario means. After the subsequent decrease and reorganization phase described above, total-AGB C again increased and approached 82–93 Mg C $ha^{-1}$ after 315–330 years, before declining at a slower pace. The maximum total-AGB C that was observed across the landscape increased over the first 100 years after which it ranged from 139 to 148 Mg C $ha^{-1}$. Dead biomass increased in proportion with AGB (~10–20 % live AGB) across scenarios and was thus highest for the least disturbed, control scenario.

Forest species composition was more stable within GRSF boundaries than without (Fig. C3, Appendix C). As one management goal was maintenance of several declining species, this is an interesting result. *P. strobus* appeared to increase equally well within GRSF, where some harvests favored its release, as it did in the absence of management. Although *Q. velutina*, *Q. montana*, and *Q. coccinea* decreased less on the managed lands, all three species declined in dominance. In general, early successional, shade-intolerant species that were rare in the initial landscape declined or disappeared under the tested disturbance regimes.

### 3.3. Defoliation effects on aboveground biomass (AGB)

The combined defoliation scenario, FTC + SM, resulted in the lowest average total-AGB of 165 Mg $ha^{-1}$ (Table 3) compared to 184 Mg $ha^{-1}$ under the control scenario with only harvest and wind disturbance. Mean AGB from all defoliation scenarios differed significantly from the control and each other (Table 3), though differences between the control and FTC were marginal (1.78 Mg/ha, lower 99.9 % CI). Annual aboveground biomass increment (AGBi) in terms of carbon declined from + 1 Mg C $ha^{-1}$ $yr^{-1}$ in the first century to a minimum of −0.5 Mg C $ha^{-1}$ $yr^{-1}$ (Fig. 7b). In the last 250 years biomass increment fluctuated slowly around 0 Mg C $ha^{-1}$ $yr^{-1}$. Mean AGBi did not differ significantly among disturbance regimes.

### 3.4. Defoliation effects on the abundance of SM hosts

GRSF forests were dominated by oaks and other tree species preferred by SM at the start of the simulation (year 2000), both in terms of mean AGB (67 % in preferred hosts) and the area of forests dominated by host species (>80 % of the landscape) (Fig. 8, Appendix C, Fig. C2). This reflects both the breadth of the SM diet (>300 woody species) (Liebhold et al., 1995), and the prevalence of oak in the study area and the eastern US (Reinmann and Hutyra, 2017).

Over the first 50 years, the relative abundance of hosts that are preferred by or resistant to SM changed very little, regardless of disturbance scenario, because of the legacy of the initial forest composition (Fig. 8, Appendix C, Fig. C2). After 200 years, the area of forest dominated by species resistant to SM had increased significantly, to between 28 % of the landscape (FTC + SM) or over 50 % (control). Hosts resistant to SM increased further to 55 % dominance of the forest area over the final 200 years for the control scenario that excluded defoliation, and just exceeded 50 % by the end of the FTC scenario. Under more intense SM defoliation regimes, SM-resistant hosts only attained dominance over 30–35 % of the landscape.

Some tree species that were resistant to SM defoliation increased in abundance regardless of the disturbance regime, but the increase was significantly lower in scenarios where SM outbreaks occurred. Changes in individual tree-species abundance shed some light on the processes leading to compositional change (Appendix C, Fig. C3). Dominance of oak species was lower after 200 years than in the initial forest (first 100 years). The resistant and immune species that increased the most over the course of the simulation were *P. strobus, Acer saccharum* Marshall 1785*, A. rubrum* L. 1753*,* and *Fraxinus americana* L. 1753*.* The combined difference in *P. strobus* and *A. saccharum* AGB between non-SM and SM scenarios approaches the 14–20 Mg $ha^{-1}$ difference observed between scenario means for total-AGB. At least one preferred species, *Tilia americana* L. 1753*,* also increased in AGB. All of these species tend to be more shade tolerant than modeled *Quercus* species, giving them the opportunity to establish and grow under the moderate disturbance regimes resulting from harvest and wind. Yet even in the absence of other stand replacing disturbances, *Quercus* species maintained a significant

**Table 3**
Mean difference and 99.9 % confidence intervals (CIs) in total biomass (live + dead AGB) among disturbance scenarios. Because harvest and wind occurred in all scenarios, the Harvest scenario is treated as the control and differences show value of the control minus defoliation scenario means over replicates of 400 year simulations.

| | Mean difference (Mg $ha^{-1}$) (lower 99.9 CI, upper 99.9 CI) | | | |
|---|---|---|---|---|
| Scenario | harvest | FTC | SM | FTC+SM |
| Harvest | 0 | – | – | – |
| FTC | 4.03 (1.78,6.27) | 0 | – | – |
| SM | 14.44 (12.20,16.68) | 10.41 (8.17,12.65) | 0 | – |
| FTC+SM | 19.15 (16.91,21.39) | 15.13 (12.89,17.37) | 4.71 (2.47,6.95) | 0 |

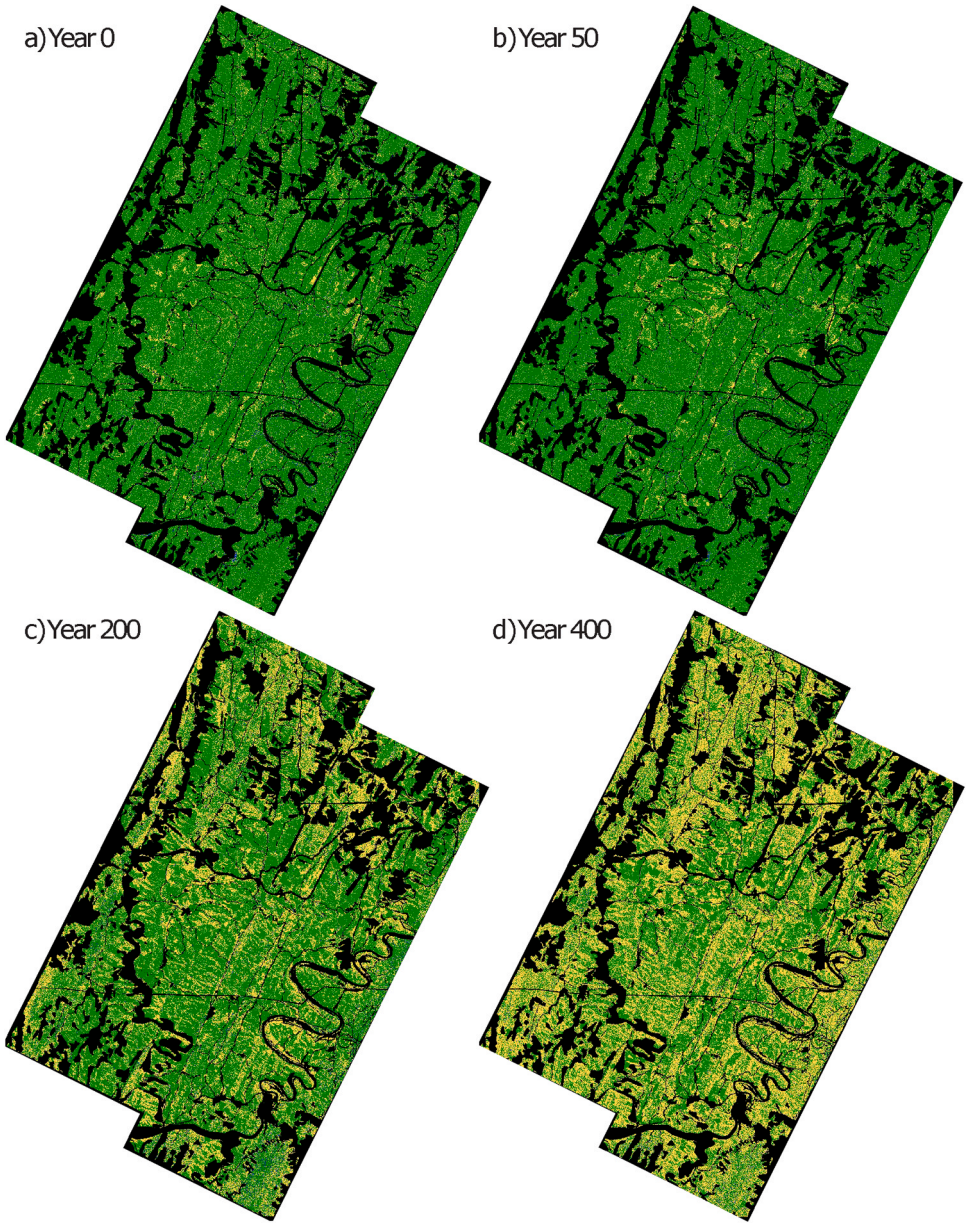


**Fig. 8.** Forests dominated by tree species that are preferred SM hosts (green), resistant hosts (gold) or immune hosts (blue) over a single SM simulation replicate. The initial forest parameterized by inventory data from 2000 shows a matrix dominated by preferred SM hosts (a). Conditions change little in the first 50 years (b), but gradually the amount of less preferred hosts increases (to 36 %) (d), largely due to increases in more shade-tolerant species.

proportion of landscape AGB, in part because harvest prescriptions were designed to favor oak regeneration. Prominent species that declined after the first 100 years to less than half of their original biomass in all scenarios included *Carya glabra* (Mill.) Sweet 1826, *Q. velutina* and *Q. coccinea*. These species are less tolerant of moderate shade and may require more severe disturbance regimes to successfully establish and compete in this landscape. Species composition changes under FTC defoliation differed very little from the control scenario.

### 3.5. Sensitivity to input parameters

Aboveground biomass (and therefore C), forest age and mean defoliation response variables were most sensitive to a shortening of the period between outbreaks (Appendix C, Table C4). Biomass response variables were also generally sensitive to the initial area of a defoliation event, which tended to propagate over the course of an outbreak (Fig. 5) and was constrained by the underlying spatial distribution of host and non-host tree species. Intensity of defoliator outbreaks was sensitive to the heterogeneity in susceptibility class among the species present in the landscape. The largest defoliation-driven changes in biomass or age structure occurred when forests were homogenous with respect to susceptibility or mortality rates, i.e. when forests were composed of only the least susceptible host species they experienced lower defoliation and mortality which led to higher AGB, or when forests were composed of only species that suffered the highest mortality rates in response to defoliation, which caused mean AGB and mean age to go down (Table C4). Simulation response variables (other than median cohort age) were not sensitive to shortening the harvest rotation period from 100 to 80 years, but AGB response pools did increase significantly if rotation periods were lengthened to 120 years (Table C4).

## 4. Discussion

Our simulation modeling experiment confirmed that introduction of

periodic SM defoliation significantly reduced landscape-mean aboveground biomass over a 75–400 year span. This result complements prior shorter simulations in the region that included SM and FTC along with other disturbances in the context of chestnut restoration (Gustafson et al., 2017, 2018). All the disturbance scenarios suggested that forests of GRSF have the potential to remain carbon sinks for 25–50 years (~2050–2075). The rate of C accumulation did not vary among scenarios but was driven most strongly by changing patterns in forest composition and age associated with forest succession, rather than with the moderate severity disturbances that we simulated. The persistent successional patterns that lowered peak C-stocks in the next forest generation also weakened GRSF's potential to act as a C sink in the future. The fact that succession was more influential than disturbances has been reported in other simulation studies (Loudermilk et al., 2013, Wang et al., 2015, Olson et al., 2021, Robbins et al., 2024) and suggests that these forests are responding more to the absence or legacy of a disturbance regime than they are to the addition of weaker disturbances than those that restructured regional forests in the decades around 1900. In other words, although forests in this landscape will respond to novel insect and harvest regimes going forward, the types of harvests and defoliators tested here did not provide the extensive stand-replacing disturbance caused by logging and fire from the 1890s to the 1930s that established the current forest (Mash, 1996). The result that moderate disturbance from SM and FTC reduced the shift from oaks to more shade-tolerant species was an unexpected result that illustrates the need to consider multiple interacting disturbances when predicting compositional change (Lucash et al., 2018).

Differences in live biomass were larger and more variable over time than differences in total biomass, because defoliator outbreaks transferred biomass from live to dead pools, where the dead biomass decayed on site. The amount of dead biomass was sensitive to changes in disturbance characteristics, but the rate of decay and layering of disturbance mortality on top of larger mortality trends driven by cohort senescence and succession buffered changes in total aboveground biomass. This indicates that empirical studies that estimate defoliation severity over the short-term may overestimate effects if only live AGB pools are measured. The lasting effect of recurrent SM disturbance was to significantly lower total biomass and shorten the potential time that disturbed forests act as carbon sinks. If a warming climate changes wood decay at rates that differ from changes in tree growth (Russell et al., 2014, Chagnon et al., 2022) the potential C sink in mid-Atlantic oak forests may disappear sooner than our simulations suggest.

Temporal changes in modeled AGBi agree with general models of ecosystem development that predict AGB accumulation in mature forests that eventually reach a "steady state" close to zero net uptake (Bormann and Likens, 1979). The GRSF landscape departs from these predictions when it shifts from being a net aboveground C sink, to a potential C source within the first 100 years and the sink does not reach equivalent strength in the following 200 years. The simulated means of AGB of 145.2 Mg ha$^{-1}$ in the year 2000 and mean AGBi ~ 1.75–2 Mg ha$^{-1}$ yr$^{-1}$ over the first 10 years, are consistent with AGB and AGBi values reported for similar temperate forests of the eastern U.S. AGBi for forest mixes of *Quercus* and *Pinus* in more xeric New Jersey pine barrens ranged from 0.69 Mg ha$^{-1}$ yr$^{-1}$ to 1.74 Mg ha$^{-1}$ yr$^{-1}$ in 2005, just prior to a SM outbreak (Clark et al., 2010). Empirical rates of AGBi accumulation increased with stand age to an asymptote of approximately 2.4 Mg ha$^{-1}$ yr$^{-1}$ for Michigan forests measured with FIA data (Caspersen et al., 2000), averaged 1.5–2 Mg ha$^{-1}$ yr$^{-1}$ for oak-pine and oak-hickory forests in another FIA analysis (He et al., 2012) and between 2 and 3 Mg ha$^{-1}$ yr$^{-1}$ for 100–150 year old deciduous forests in eastern Maryland (Foster et al., 2010, McMahon et al., 2010). Total mean AGB peaked at GRSF between 206 and 225 Mg ha$^{-1}$ depending on disturbance regime, very close to biome-wide estimates for temperate deciduous sites of 218 Mg ha$^{-1}$ reviewed by Luyssaert et al. (2007). These aboveground biomass estimates are also consistent with comprehensive analyses of FIA data that reported AGB values of 100–250 Mg ha$^{-1}$ for the mature oak and pine mixes common in GRSF (Jenkins et al., 2001, Lichstein et al., 2009). GRSF AGB peaked at a level similar to oak-pine mixes in Arkansas simulated by Wang et al. (2013) and lower than the AGB of 245 Mg ha$^{-1}$ measured for mesic northern hardwood forests at Hubbard Brook Experimental Forest in New Hampshire that are older and more stable than those at GRSF (van Doorn et al., 2011). GRSF AGB accumulation did not stop aggrading until 50–75 years after the simulation started in 2000.

Research on forest response to SM outbreaks has consistently predicted that stand composition will shift away from the most susceptible host species towards those that are more resistant (Campbell and Sloan, 1977, Gansner et al., 1983, Davidson et al., 1999, Muzika and Liebhold, 1999). Our landscape simulations indicate that some of these compositional shifts would be expected due to succession, stand dynamics, human management and fire suppression alone. Introduced SM defoliation tended to lessen the strength of some successional trends, specifically slowing the spread and ingrowth of shade tolerant species *P. strobus* and *A. saccharum*, presumably due to higher defoliation that occurred on less preferred hosts growing in proximity to preferred hosts during the longest outbreaks. Moderate SM defoliation in conjunction with targeted management may retain some SM host species. The GRSF landscape may be unusually resistant to the compositional changes often associated with SM, possibly due to shallow, acidic soils that are not easily colonized by *Acer* species, and the rain shadow cast by the Allegheny Plateau to the West. The local dominance of *Quercus* and *Pinus* pollen dating back over 7000 years supports this speculation, though the pattern appears likely to change with continued fire suppression (Brown and Townsend, 2004, Nowacki and Abrams, 2008).

The outbreak characteristics of the simulated defoliators offer some ecological insights into the type of defoliator disturbances that most affect C storage in mixed oak forests. The sensitivity of aboveground biomass to shorter periods between outbreaks was consistent with a non-spatial simulation model (Medvigy et al., 2012) and suggests that environmental trends or ecological interactions that speed up outbreak periodicity would be of particular concern to forest C stocks. The intensity of defoliator outbreaks was sensitive to the spatial heterogeneity of preferred hosts across the landscape. This suggests that interactions between defoliator host-preference and the distributions of tree species are important to understand long-term forest response. Forest biomass and age were insensitive to growth effects caused by defoliation, showing that changes caused by mortality were large enough to overwhelm effects of growth alone, in contrast to estimates in other defoliator systems (Benoit and Lachance, 1990).

### 4.1. Model limitations

Simulating multiple ecological outcomes under possible disturbance regimes illustrates a range of potential future states for oak forests in the US central hardwoods region. This range of potential forest structure and composition depends on appropriate model design, parameterization, inputs and interpretation. Our simulations assumed that many of the forest dynamics observed today will continue into the future. This assumption simplified the parameter space and allowed us to focus on specific questions surrounding defoliation effects on forests and potential disturbance interactions. However, many of the dynamics and processes incorporated into the model have the potential to change over time. Rates of tree species establishment, growth, and mortality may vary under a changing climate (see Gustafson et al., 2017, 2018), as may defoliator population dynamics (e.g., Tobin et al., 2014). Temporal patterns of defoliator outbreaks can also be sensitive to the abundance of hosts in the landscape (Haynes et al., 2009, Cooke et al., 2024), and the amplitude and periodicity of invasive outbreaks can change dramatically over centuries (Liebhold et al., 2022). Other invasive insects that are killing important species that are not hosts of SM and FTC were not modeled, such as emerald ash borer (*Agrilus planipennis* Obenberger) and hemlock wooly adelgid (*Adelges tsugae* Anand 1928). Soil nutrient

cycling and soil carbon are also subject to global change and were not included in this research (McNeil et al., 2007). Prescribed fires or fires that escape suppression would provide important regeneration environments for the persistence of some species that were virtually eliminated from GRSF over time, such as *Q. coccinea*, *P. rigida*, *Prunus serotina*, or *Liriodendron tulipifera L.* Our simulation results should be considered in light of the uncertainty surrounding these changing factors.

## 5. Conclusions

Invasive spongy moth populations continue to spread into new forested regions of the eastern US and their potential effects on oak-hickory forests of the central hardwoods region continue to cause concern. Simulations with the 'Biomass Insects' defoliation model showed that a typical mixed-oak forest of this region should continue to show a net increase in woody increment until ~2050–2075, allowing it to act as a sink for atmospheric C, in spite of the active management, wind, SM and FTC defoliation disturbance tested here. Beyond that time range, C uptake for the landscape weakened and was predicted to oscillate near zero.

While trends in biomass increment were driven more by forest age and successional processes, defoliation by invasive SM significantly reduced aboveground biomass and standing wood, with more pronounced short-term effects on live biomass and species composition than on total aboveground biomass. Defoliation also changed trends in forest composition, most surprisingly by interfering with successional increases of shade tolerant species such as *P. strobus* and *A. saccharum*, even though they were less preferred by SM, likely due to elevated defoliation that occurred when these species grew in mixtures or in proximity with more preferred oaks. Invasive SM outbreaks differed from native FTC outbreaks, causing reductions in biomass that were 39 % larger than reductions caused by FTC alone. Given that today's mid-Atlantic oak forests are the product of the massive logging, fire and then fire suppression that occurred nearly 150 years ago, the addition of moderate to severe SM defoliation outbreaks showed potential to favor more intolerant oak species that lack regeneration avenues under less intense disturbance regimes.

Determining how temporal dynamics of defoliator outbreaks will respond to changing environmental trends remains a vexing and complex research need. Our simulations indicate that potential changes to defoliator outbreaks that could change forest structure the most would be adaptations that change host breadth of SM or FTC over time, or changes in the defoliator disease complex that contributes to insect outbreak population collapse and may lead to significantly shorter or less frequent outbreaks.

## Data statement

The 'Biomass Insects' Defoliation model and underlying code are open source and freely available on Github: https://github.com/LANDIS-II-Foundation/Extension-Biomass-Insects.git via the LANDIS-II repository. As annual LANDIS-II model inputs and outputs can be very large, a temporal subset will be made available via a data package on a site that allows large data sets. Additional data associated with this research are available on request.

## CRediT authorship contribution statement

**Mladenoff David J:** Writing – review & editing, Supervision, Resources, Project administration, Methodology, Funding acquisition, Conceptualization. **Sturtevant Brian R:** Writing – review & editing, Resources, Project administration, Funding acquisition, Conceptualization. **Scheller Robert M:** Writing – review & editing, Supervision, Software, Resources, Methodology, Conceptualization. **Brian Miranda:** Writing – review & editing, Software, Resources, Methodology. **Townsend Philip A:** Writing – review & editing, Supervision, Project administration, Methodology, Funding acquisition, Conceptualization. **Foster Jane R:** Writing – review & editing, Writing – original draft, Visualization, Software, Methodology, Funding acquisition, Formal analysis, Data curation, Conceptualization.

## Funding

This work was supported by NASA Carbon Cycle Science grant [NNX06AD45G] and NASA earth system science graduate fellowship [NNX08AU93H] and the USDA Forest Service Southern and Northern Research Stations. The findings and conclusions in this publication are those of the authors and should not be construed to represent any official USDA or U.S. Government determination or policy.

## Declaration of Competing Interest

The authors declare that they have no known competing financial interests or personal relationships that could have appeared to influence the work reported in this paper.

## Acknowledgements

M. Beals (forest manager, Green Ridge State Forest) and F. Zumbrun (former forest manager, GRSF) generously shared time, advice, and data for the forest including harvest maps and forest management plans. We thank M. Turner (UW-Madison), K. Raffa (UW-Madison), and C. Lorimer (UW-Madison) for input on experimental design and feedback on earlier versions of this manuscript.

## Appendix A. Supporting information

Supplementary data associated with this article can be found in the online version at doi:10.1016/j.foreco.2025.123450.

## References

Aber, J.D., Federer, C.A., 1992. A generalized, lumped-parameter model of photosynthesis, evapotransipiration and net primary production in temperate and boreal forest ecosystems. Oecologia 92, 463–474.
Allen, C.D., 2007. Interactions across spatial scales among forest dieback, fire and erosion in northern New Mexico landscapes. Ecosystems 10, 797–808.
Allstadt, A.J., Liebhold, A.M., Johnson, D.M., Davis, R.E., Haynes, K.J., 2015. Temporal variation in the synchrony of weather and its consequences for spatiotemporal population dynamics. Ecology 96, 2935–2946.
Benoit, P., and Lachance, D. 1990. Gypsy moth in Canada: Behavior and control. Ottawa, ON, Canada.
Bormann, F.H., Likens, G.E., 1979. Catastrophic disturbance and the steady-state in Northern hardwood forests. Am. Sci. 67, 660–669.
Brown, R.W., and Townsend, P.A. 2004. Vegetation history from two rare wetland sites in Western Maryland. Final Report to the MD/DC Chapter of the Nature Conservancy, Bethesda, MD.
Campbell, R.W., Sloan, R.J., 1977. Forest stand response to defoliation by gypsy moth. For. Sci. 1–34.
Caspersen, J.P., Pacala, S.W., Jenkins, J.C., Hurtt, G.C., Moorcroft, P.R., Birdsey, R.A., 2000. Contributions of land-use history to carbon accumulation in U.S. forests. Science 290, 1148–1151.
Chagnon, C., Moreau, G., Bombardier-Cauffopé, C., Barrette, J., Havreljuk, F., Achim, A., 2022. Broad-scale wood degradation dynamics in the face of climate change: a meta-analysis. GCB Bioenergy 14 (8), 941–958. https://doi.org/10.1111/gcbb.12951.
Clark, K.L., Skowronski, N., Hom, J., 2010. Invasive insects impact forest carbon dynamics. Glob. Change Biol. 16, 88–101.
Cook, B.D., Bolstad, P.V., Martin, J.G., Heinsch, F.A., Davis, K.J., Wang, W., Desai, A.R., Teclaw, R.M., 2008. Using light-use and production efficiency models to predict photosynthesis and net carbon exchange during forest canopy disturbance. Ecosystems 11, 26–44.
Cooke, B.J., Lorenzetti, F., Roland, J., 2009. On the duration and distribution of forest tent caterpillar outbreaks in east-central Canada. J. Èntomol. Soc. Ont. 140, 3–18.
Cooke, B.J., Lorenzetti, F., 2006. The dynamics of forest tent caterpillar outbreaks in Quebec, Canada. For. Ecol. Manag. 226, 110–121.
Cooke, B.J., Nealis, V.G., Regniere, J., 2007. Insect defoliators as periodic disturbances in northern forest ecosystems. In: Johnson, E.A., Miyanishi, K. (Eds.), Plant Disturbance Ecology: The Process and The Response. Academic Press, Burlington, pp. 487–525.
Cooke, B.J., Robert, L., Sturtevant, B.R., Kneeshaw, D., Thapa, B., 2024. Confronting the cycle synchronisation paradigm of defoliator outbreaks in space and time—evidence from two systems in a mixed-species forest landscape. J. Ecol. 112, 152–173.

Crow, G.R., Hicks, R.R., 1990. Prediction mortality in mixed oak stands following spring insect defoliation. For. Sci. 36, 831–841.
Davidson, C.B., Gottschalk, K.W., Johnson, J.E., 1999. Tree mortality following defoliation by the European gypsy moth (*Lymantria dispar* L.) in the United States: a review. For. Sci. 45, 74–84.
Davis, S.C., Hessl, A.E., Scott, C.J., Adams, M.B., Thomas, R.B., 2009. Forest carbon sequestration changes in response to timber harvest. For. Ecol. Manag. 258, 2101–2109.
Dye, A., Barker Plotkin, A., Bishop, D., Pederson, N., Poulter, B., Hessl, A., 2016. Comparing tree-ring and permanent plot estimates of aboveground net primary production in three eastern U.S. forests. Ecosphere, e01454.
Fei, S., Morin, R.S., Oswalt, C.M., Liebhold, A.M., 2019. Biomass losses resulting from insect and disease invasions in US forests. Proc. Natl. Acad. Sci. 201820601.
Fisher, R.A., Muszala, S., Verteinstein, M., Lawrence, P., Xu, C., McDowell, N.G., Knox, R. G., Koven, C., Holm, J., Rogers, B.M., Spessa, A., Lawrence, D., Bonan, G., 2015. Taking off the training wheels: the properties of a dynamic vegetation model without climate envelopes, CLM4.5(ED). Geosci. Model Dev. 8 (11), 3593–3619.
Foster, J.R. 2011. Forest insect defoliation patterns and carbon dynamics: Linking remote sensing with simulation models. Dissertation, University of Wisconsin-Madison.
Foster, J.R., 2017. Xylem traits, leaf longevity and growth phenology predict growth and mortality response to defoliation in northern temperate forests. Tree Physiol. 37 (9), 1151–1165.
Foster, J.R., Burton, J.I., Forrester, J.A., Liu, F., Muss, J.D., Sabatini, F.M., Scheller, R.M., Mladenoff, D.J., 2010. Evidence for a recent increase in forest growth is questionable. Proc. Natl. Acad. Sci. 107, E86–E87.
Foster, J.R., Townsend, P.A., Mladenoff, D.J., 2013. Spatial dynamics of a gypsy moth defoliation outbreak and dependence on habitat characteristics. Landsc. Ecol. https://doi.org/10.1007/s10980-013-9879-8.
Frey, B.R., Lorenzetti, F., Despland, E., 2023. Forest tent caterpillar outbreaks restructure hardwood forest regeneration and productivity. For. Ecol. Manag. 545, 121234. https://doi.org/10.1016/j.foreco.2023.121234.
Gansner, D.A., Herrick, O.W., Debald, P.S., Acciavatti, R.W., 1983. Changes in forest condition associated with gypsy-moth. J. For. 81, 155–157.
Gustafson, E.J., de Bruijn, A., Lichti, N., Jacobs, D.F., Sturtevant, B.R., Foster, J., Miranda, B.R., Dalgleish, H.J., 2017. The implications of American chestnut reintroduction on landscape dynamics and carbon storage. Ecosphere 8 (4), e01773. https://doi.org/10.1002/ecs2.1773.
Gustafson, E.J., Shvidenko, A.Z., Sturtevant, B.R., Scheller, R.M., 2010. Predicting global change effects on forest biomass and composition in south-central Siberia. Ecol. Appl. 20, 700–715.
Gustafson, E.J., Sturtevant, B.R., de Bruijn, A.M.G., et al., 2018. Forecasting effects of tree species reintroduction strategies on carbon stocks in a future without historical analog. Glob. Change Biol. 24, 5500–5517. https://doi.org/10.1111/gcb.14397.
Haynes, K.J., Liebhold, A.M., Johnson, D.M., 2009. Spatial analysis of harmonic oscillation of gypsy moth outbreak intensity. Oecologia 159, 249–256. https://doi.org/10.1007/s00442-008-1207-7.
He, L., Chen, J.M., Pan, Y., Birdsey, R., Kattge, J., 2012. Relationships between net primary productivity and forest stand age in U.S. forests. Glob. Biogeochem. Cycles 26. GB3009.
Herms, D.A., Mattson, W.J., 1992. The dilemma of plants: to grow or defend. Q. Rev. Biol. 67, 283–335.
Houghton, R.A., 2005. Aboveground forest biomass and the global carbon balance. Glob. Change Biol. 11, 945–958.
James, P.M.A., Fortin, M.J., Fall, A., Kneeshaw, D., Messier, C., 2007. The effects of spatial legacies following shifting management practices and fire on boreal forest age structure. Ecosystems 10, 1261–1277.
Jenkins, J.C., Birdsey, R.A., Pan, Y., 2001. Potential biomass and NPP estimation for the Mid-Atlantic region (USA) using forest inventory data. Ecol. Appl. 11, 1174–1193.
Johnson, D.M., Liebhold, A.M., Bjornstad, O.N., 2006. Geographical variation in the periodicity of gypsy moth outbreaks. Ecography 29, 367–374.
Johnson, D.M., Liebhold, A.M., Bjornstad, O.N., McManus, M.L., 2005. Circumpolar variation in periodicity and synchrony among gypsy moth populations. J. Anim. Ecol. 74, 882–892.
Kretchun, A.M., Scheller, R.M., Lucash, M.S., Clark, K.L., Hom, J., Van Tuyl, S., 2014. Predicted effects of gypsy moth defoliation and climate change on forest carbon dynamics in the New Jersey Pine Barrens. PLoS One 9 (8), e102531.
Lichstein, J.W., Wirth, C., Horn, H.S., Pacala, S.W., 2009. Biomass chronosequences of United States forests: implications for carbon storage and forest management. In: Wirth, C., Gleixner, G., Heimann, M. (Eds.), Old-growth forests:function, fate and value. Ecological Studies, 207. Springer-Verlag, Berlin, Heidelberg, pp. 301–341.
Liebhold, A.M., Brockerhoff, E.G., McCullough, D.G., 2023. Forest insect invasions and their management. For. Entomol. Pathol. 1, 789–810.
Liebhold, A.M., Gottschalk, K.W., Muzika, R., Montgomery, M.E., Young, R., O'Day, K., Brooks, K. 1995. Suitability of North American tree species to the gypsy moth: A summary of field and laboratory tests. General Technical Report NE-211. Radnor, PA: USDA Forest Service.
Liebhold, A.M., Hajek, A.E., Walter, J.A., Haynes, K.J., Elkinton, J., Muzika, R.-M., 2022. Historical change in the outbreak dynamics of an invading forest insect. Biol. Invasions 24, 879–889.
Loudermilk, E.L., Scheller, R.M., Weisberg, P.J., Yang, J., Dilts, T., Karam, S.L., Skinner, C.N., 2013. Carbon dynamics in the future forest: the importance of climate-fire interactions and long-term successional legacy. Glob. Change Biol. 19, 3502–3515.
Lovett, G.M., Weiss, M., Liebhold, A.M., Holmes, T.P., Leung, B., Lambert, K.F., Orwig, D. A., Campbell, F.T., Rosenthal, J., McCullough, D.G., Wildova, R., Ayres, M.P., Canham, C.D., Foster, D.R., LaDeau, S.L., Weldy, T., 2016. Nonnative forest insects and pathogens in the United States: impacts and policy options. Ecol. Appl. 26 (5), 1437–1455. https://doi.org/10.1890/15-1176.
Lucash, M.S., Scheller, R.M., Sturtevant, B.R., Gustafson, E.J., Kretchun, A.M., Foster, J. R., 2018. More than the sum of its parts: how disturbance interactions shape forest dynamics under climate change. Ecosphere 9 (6), e02293.
Luyssaert, S., Inglima, I., Jung, M., Richardson, A.D., et al., 2007. CO2 balance of boreal, temperate, and tropical forests derived from a global database. Glob. Change Biol. 13, 2509–2537.
MacLean, D.A., 1980. Vulnerability of spruce stands during uncontrolled spruce budworm outbreaks – a review and discussion. For. Chron. 56, 213–221.
Man, R., Rice, J.A., 2010. Response of aspen stands to forest tent caterpillar defoliation and subsequent overstory mortality in northeastern Ontario, Canada. For. Ecol. Manag. 260, 1853–1860.
Mash, J. 1996. The Land of the Living: The Story of Maryland's Green Ridge Forest. Commercial Press, Cumberland, Maryland.
Mason, C.J., McManus, M.L., 1981. Larval dispersal of the gypsy moth In. In: Doane, C.C., McManus, M.L. (Eds.), The Gypsy Moth: Research Toward Integrated Pest Management, 1584. U.S. Department of Agriculture Technical Bulletin, pp. 161–202.
McCullough, D.G., 2000. A review of factors affecting the population dynamics of jack pine budworm (*Choristoneura pinus pinus* Freeman). Popul. Ecol. 42, 243–256.
McMahon, S.M., Parker, G.G., Miller, D.R., 2010. Evidence for a recent increase in forest growth. Proc. Natl. Acad. Sci. 107, 3611–3615.
McNeil, B.E., de Beurs, K.M., Eshleman, K.N., Foster, J.R., Townsend, P.A., 2007. Maintenance of ecosystem nitrogen limitation by ephemeral forest disturbance: an assessment using MODIS, Hyperion, and Landsat ETM+. Geophys. Res. Lett. 34. L19406.
Medvigy, D., Clark, K.L., Skowronski, N.S., Schafer, K.V.R., 2012. Simulated impacts of insect defoliation on forest carbon dynamics. Environ. Res. Lett. 7, 045703.
Mladenoff, D.J., 2004. LANDIS and forest landscape models. Ecol. Model. 180, 7–19.
Mladenoff, D., Host, G., Boeder, J., Crow, T., 1996. LANDIS A spatial model of forest landscape disturbance, succession and management. In: Goodchild, M.F., Steyaert, L. T., Parks, B.O., Johnston, C., Maidment, D., Crane, M., et al. (Eds.), *GIS and Environmental Modeling: Progress and Research Issues*. GIS World Books, Ft. Collins, CO, pp. 175–179..
Mladenoff, He, 1999. Design, behavior and application of LANDIS, an object-oriented model of forest landscape disturbance and succession. In: Mladenoff, D.J., Baker, W. L. (Eds.), Spatial Modelling of Forest Landscape Change: Approaches and Applications. Cambridge University Press, Cambridge, UK, pp. 125–162.
Muzika, R.M., Liebhold, A.M., 1999. Changes in radial increment of host and nonhost tree species with gypsy moth defoliation. Can. J. For. Res. 29, 1365–1373.
Niemelä, P., Mattson, W.J., 1996. Invasion of North American Forests by European Phytophagous Insects: Legacy of the European crucible? Bioscience 46 (10), 741–753.
Nowacki, G.J., Abrams, M.D., 2008. The demise of fire and "mesophication" of forests in the eastern United States. BioScience 58 (2), 123–138.
Olson, S.K., Smithwick, E.A.H., Lucash, M.S., Scheller, R.M., Nicholas, R.E., Ruckert, K. L., Caldwell, C.M., 2021. Landscape-scale forest reorganization following insect invasion and harvest under future climate change scenarios. Ecosystems 24, 1756–1774. https://doi.org/10.1007/s10021-021-00616-w.
Pan, Y., Birdsey, R.A., Fang, J.Y., Houghton, R., Kauppi, R.E., Kurz, W.A., Phillips, O.L., Shvidenko, A., Lewis, S.L., Canadell, J.G., Ciais, P., Jackson, R.B., Pacala, S.W., McGuire, A.D., Piao, S.L., Rautiainen, A., Sitch, S., Hayes, D., 2011. A large and persistent carbon sink in the world's forests. Science 333, 988–993.
Pan, Y., Birdsey, R.A., Homm, J., McCullough, K., 2009. Separating effects of changes in atmospheric composition, climate and land-use on carbon sequestration of U.S. Mid-Atlantic temperate forests. For. Ecol. Manag. 259, 151–164.
Parry, D., Goyer, R.A., 2004. Variation in the suitability of host tree species for geographically discrete populations of forest tent caterpillar. Environ. Entomol. 33, 1477–1487.
Pastor, J. and Post, W.M. 1985. Development of a linked forest productivity-soil process model. Oak Ridge, Tennessee, USA: Oak Ridge National Laboratory; ORNL/TM-9519.
Peltonen, M., Liebhold, A.M., Bjoernstad, O.N., Willliams, D.W., 2002. Spatial synchrony in forest insect outbreaks: Roles of regional stochasticity and dispersal. Ecology 83, 3120–3129.
Peltzer, D.A., Allen, R.B., Lovett, G.M., Whitehead, D., Wardle, D.A., 2010. Effects of biological invasions on forest carbon sequestration. Glob. Change Biol. 16, 732–746.
Pennsylvania Department of Conservation and Natural Resources. (n.d.). Forest Health Fact Sheet: Forest Tent Caterpillar. Bureau of Forestry, Division of Forest Pest Management. Retrieved from ⟨https://elibrary.dcnr.pa.gov⟩.
Peters, D.P.C., Pielke, R.A., Bestelmeyer, B.T., Allen, C.D., Munson-McGee, S., Havstad, K.M., 2004. Cross-scale interactions, nonlinearities, and forecasting catastrophic events. Proc. Natl. Acad. Sci. USA 101, 15130–15135.
Picotte, J.J., Bhattarai, K., Howard, D., Lecker, J., Epting, J., Quayle, B., Benson, N., Nelson, K., 2020. Changes to the Monitoring Trends in Burn Severity program mapping production procedures and data products. Fire Ecol. 16 (1), 1–12.
Pinkard, E.A., Battaglia, M., Roxburgh, S., O'Grady, A.P., 2011. Estimating forest net primary production under changing climate: adding pests to the equation. Tree Physiol. 31, 686–699.
Quirion, B.R., Domke, G.M., Walters, B.F., Lovett, G.M., Fargione, J.E., Greenwood, L., Serbesoff-King, K., Randall, J.M., Fei, S., 2021. Insect and disease disturbances correlate with reduced carbon sequestration in forests of the contiguous United States. Front. For. Glob. Change 4, 716582. https://doi.org/10.3389/ffgc.2021.716582.

Reardon, R., Venables, L., Roberts, A. 1993. The Maryland integrated pest management gypsy moth project 1983–1987. NA-TP-07-93. Radnor, PA: U.S. Department of Agriculture, Forest Service, Northeastern Area. 35 p.

Reese, G.C., Sturtevant, B.R., Dymond, C.C., Quigley, K.M., Duveneck, M.J., Lucash, M. S., Gustafoson, E.J., Scheller, R.M., Russell, M.B., and Miranda, B.R. (2024). Best practices for calibration of forest landscape models using fine-scaled reference information. Canadian Journal of Forest Research.

Regniere, J., Nealis, V., Porter, K., 2009. Climate suitability and management of the gypsy moth invasion into Canada. Biol. Invasions 11, 135–148.

Reinmann, A.B., Hutyra, L.R., 2017. Edge effects enhance carbon uptake and its vulnerability to climate change in temperate broadleaf forests. Proc. Natl. Acad. Sci. 114, 107–112.

Robbins, Z., Loudermilk, E.L., Mozelewski, T.G., Jones, K., Scheller, R.M., 2024. The fire regimes of the Southern Appalachians may radically shift under climate change. Fire Ecol. 20, 2.

Russell, M.B., Woodall, C.W., D'Amato, A.W., Fraver, S., Bradford, J.B., 2014. Linking climate change and downed woody debris decomposition across forests of the eastern United States. Biogeosciences 11, 6417–6425. https://doi.org/10.5194/bg-11-6417-2014.

Ryerson, D.E., Swetnam, T.W., Lynch, A.M., 2003. A tree-ring reconstruction of western spruce budworm outbreaks in the San Juan Mountains, Colorado, USA. Can. J. For. Res. 33, 1010–1028.

Scheller, R.M., Domingo, J.B., Sturtevant, B.R., Williams, J.S., Rudy, A., Mladenoff, D.J., Gustafson, E.J., 2007. Design, development, and application of LANDIS-II, a spatial landscape simulation model with flexible temporal and spatial scales. Ecol. Model. 201, 409–419.

Scheller, R.M., Mladenoff, D.J., 2004. A forest growth and biomass module for a landscape simulation model, LANDIS: design, validation, and application. Ecol. Model. 180, 211–229.

Scheller, R.M., Mladenoff, D.J., 2005. A spatially interactive simulation of climate change, harvesting, wind, and tree species migration and projected changes to forest composition and biomass in northern Wisconsin, USA. Global Change Biology 11 (2), 307–321.

Schimel, D., 2007. Carbon cycle conundrums. Proc. Natl. Acad. Sci. 104, 18353–18354.

Schowalter, T.D., 2017. Biology and management of the forest tent caterpillar (Lepidoptera: Lasiocampidae). Journal of Integrated Pest Management 8 (1). https://doi.org/10.1093/jipm/pmx022.

Sharov, A.A., Pijanowski, B.C., Liebhold, A.M., Gage, S.H., 1999. What affects the rate of gypsy moth (Lep- idoptera: Lymantriidae) spread: winter temperature or forest susceptibility? Agric. For. Entomol. 1, 37–45.

Simons-Legaard, E., Legaard, K., Weiskittel, A., 2025. Declining conifer productivity will drive future forest dynamics as climate changes in northern New England. Ecol. Appl. 35, e70028.

Soil Survey Staff, Natural Resources Conservation Service, United States Department of Agriculture. Web Soil Survey. Available online at https://websoilsurvey.nrcs.usda.gov/. Accessed [04/23/2009].

Sturtevant, B.R., Gustafson, E.J., Li, W., He, H.S., 2004. Modeling biological disturbances in LANDIS: a module description and demonstration using spruce budworm. Ecol. Model. 180, 153–174.

Thomas, S.C., Malczewski, G., 2007. Wood carbon content of tree species in Eastern China: interspecific variability and the importance of the volatile fraction. J. Environ. Manag. 85, 659–662.

Tobin, P.C., Gray, D.R., Liebhold, A.M., 2014. Supraoptimal temperatures influence the range dynamics of a non-native insect. Divers. Distrib. 20 (7), 813–823.

van Doorn, N.S., Battles, J.J., Fahey, T.J., Siccama, T.G., Schwarz, P.A., 2011. Links between biomass and tree demography in a northern hardwood forest: a decade of stability and change in Hubbard Brook Valley, New Hampshire. Can. J. For. Res. 41, 1369–1379.

Volney, W.J.A., Fleming, R.A., 2000. Climate change and impacts of boreal forest insects. Agriculture, Ecosystems & Environment 82 (1), 283–294.

Wang, W.J., He, H.S., Spetich, M.A., Shifley, S.R., Thompson, I., Larsen, D.R., Fraser, J.S., Yang, J., 2013. A large-scale forest landscape model incorporating multi-scale processes and utilizing forest inventory data. Ecosphere 4, 106.

Wang, W.J., He, H.S., Thompson, F.R., Fraser, J.S., Hanberry, B.B., Dijak, W.D., 2015. Importance of succession, harvest, and climate change in determining future forest composition in U.S. Central Hardwood Forests. Ecosphere 6, 277.

Whitehead, D., 2011. Modelling the impacts of pests on forest productivity: a pathway through complexities and conundrums. Tree Physiol. 31, 683–685.

Wood, D. 2008. Evaluating the susceptibility of sugar maple stands to defoliation by forest tent caterpillar (Malacosoma disstria Hubner) and the vulnerability to decline. Thesis, University of Michigan.

Xu, C., Gertner, G.Z., Scheller, R.M., 2012. Importance of colonization and competition in forest landscape response to global climatic change. Clim. Change 110, 53–83.